Catalysis Science & Technology

PAPER

View Article Online
View Journal | View Issue

Cite this: *Catal. Sci. Technol.*, 2015, 5, 2441

Received 2nd January 2015, Accepted 3rd February 2015

DOI: 10.1039/c5cy00004a

www.rsc.org/catalysis

Hydrogenation of succinic acid over supported rhenium catalysts prepared by the microwave-assisted thermolytic method†

Xin Di,[a] Zhengfeng Shao,[a] Chuang Li,[a] Wenzhen Li[b] and Changhai Liang*[a]

A series of metallic Re/C catalysts were prepared with the microwave-assisted thermolytic method by using decacarbonyldirhenium [$Re_2(CO)_{10}$] as a precursor for the hydrogenation of succinic acid. The results of FT-IR, UV-Vis, XRD, HRTEM, ICP, TPR and CO chemical adsorption showed that the as-prepared catalysts had well-dispersed rhenium nanoparticles on activated carbon. Changing irradiation time or rhenium loadings could effectively adjust the properties of Re/C catalysts which exhibited good catalytic performance for the hydrogenation of succinic acid. There were plenty of active sites on Re/C catalysts for the high concentration hydrogenation of succinic acid, and increasing temperature or pressure improved catalytic activity at a defined scope. From the kinetic study of succinic acid catalytic hydrogenation, there was a certain converting relationship between the different intermediates and the product distribution which could be controlled by variation of reaction time.

Introduction

Considering the rapid consumption and limited reserves of fossil fuels such as oil and gas, there is an urgent need to find alternatives to mitigate such a situation. Of all the renewable energies available today, biomass-derived energies and chemicals seem to be a good choice. According to the data released by the U.S. Department of Energy, succinic acid belongs to a new class of bio-derived building-block chemicals, which could replace the current maleic anhydride C4 platform. The production of succinic acid could achieve 20 000–30 000 tonnes per year.[1] Therefore, it is economically and technically feasible to produce more valuable chemicals using succinic acid as raw material. The succinic acid can be converted into many valuable products by hydrogenation, such as γ-butyrolactone (GBL), tetrahydrofuran (THF), 1,4-butanediol (BDO) and others.[2] All these chemicals find expansive use in many fields.[3] To name a few, THF can be used as a high-performance solvent[4,5] and GBL is an important chemical intermediate in the manufacture of pyrrolidone derivatives.[6] BDO can be a raw material for many organic syntheses, including polybutylene succinate (PBS) and polybutylene terephthalate (PBT) resins which may be used for the synthesis of films and engineering plastics. The main application of BDO is in the production of THF, which approximately contributes to 40% of the total BDO production volume.[7,8]

A series of catalysts have been developed for the hydrogenation of succinic acid. The activity of the catalysts is highly affected by metal species.[2,5,9] In fact, palladium[10–13] and ruthenium[14–16] based catalytic systems are the most studied among various hydrogenation catalysts because of their high activity and selectivity. The bimetallic catalysts exhibit different physical and chemical properties when adopting the second metal as an additive, such as Ru–Co,[17] Ru–Re,[18] Pt–Re[19] and Pd–Re[20] based catalysts. It is well known that supported rhenium catalysts can effectively reduce both carboxyl and carbonyl compounds.[21] It is reasonable to propose that rhenium-based catalysts should also have a positive effect on hydrogenation of succinic acid.[22] However, little systematic research was performed on the hydrogenation of succinic acid over supported Re catalysts.

At present, a number of preparation methods are reported for supported rhenium catalysts. However, most of the methods require the modification of the supports, and the inevitable use of solvents in the preparation process. Moreover, it is difficult to control the preparation steps and obtain highly dispersed catalysts. The microwave-assisted thermolytic method, which is generally more environmentally friendly than conventional wet preparation methods, has attracted the increasing attention of various groups for the syntheses of supported catalysts.[23–25] The microwave-assisted thermolytic method avoids the use of solvents and has a

---

[a] *Laboratory of Advanced Materials and Catalytic Engineering, Dalian University of Technology, Dalian 116024, China. E-mail: changhai@dlut.edu.cn; Fax: +86 411 84986353*

[b] *DCBE, Biorenewables Research Laboratory, Iowa State University, Iowa 50011, USA*

† Electronic supplementary information (ESI) available. See DOI: 10.1039/c5cy00004a

better heat transfer effect than conventional methods. Catalysts prepared by the microwave thermolytic method could exhibit good textural properties and show some distinct catalytic properties. For example, Ni *et al.* successfully prepared supported ruthenium catalysts by the microwave-assisted thermolytic method and the as-prepared catalysts showed superior catalytic properties in the hydrogenation of cinnamaldehyde.[26] Hence, it is expected that highly dispersed supported rhenium catalysts could also be prepared with the microwave-assisted thermolytic method.

In this work, supported rhenium catalysts were prepared with the microwave-assisted thermolytic method by using decacarbonyldirhenium [$Re_2(CO)_{10}$] as a precursor. The influence of microwave irradiation time and rhenium loadings on catalytic activity was investigated in detail. The structure and textural properties of the catalysts were characterized and discussed with their catalytic performance in the aqueous phase hydrogenation of bio-derived succinic acid. Meanwhile, the kinetics of succinic acid catalytic hydrogenation was also investigated.

Experimental

Catalyst preparation

Re nanoparticles on activated carbon [C] (surface area: 1502 $m^2\ g^{-1}$, pore volume: 0.7 $cm^3\ g^{-1}$, pore diameter: 1.9 nm) catalysts were prepared with the microwave-assisted thermolytic method using decacarbonyldirhenium [$Re_2(CO)_{10}$] (>99.9%, Acros Organics Co. Ltd., USA) as a precursor. Before the preparation of catalysts, the active carbon was pre-treated with HNO_3 (10 M) for 4 h at 90 °C. $Re_2(CO)_{10}$ and active carbon were simultaneously added into an agate mortar and then mechanically mixed for 20 min. The homogeneous mixture was transferred into a fluidized quartz tube reactor which was then put in a microwave reactor. The homogeneous mixture was fluidized with argon for 2 h at room temperature to make sure that the reaction mixture was kept under an inert atmosphere. Afterwards, the microwave reactor was set at 2.45 GHz with a power of 800 W and then kept for certain minutes. Finally, the resultants were cooled to room temperature under argon. The catalysts prepared with different microwave irradiation times and the same Re loading (4.0 wt.%) were identified as Re/C-*X* (*X* = 1, 3, 4, 5, 7, 10 and 15), where *X* represents microwave irradiation time. Adjusting the ratio of $Re_2(CO)_{10}$ to C, a series of catalysts with different Re loadings and the same irradiation time (5 min) could be prepared. These catalysts were identified as Re/C-*Y*% (*Y* = 2, 3, 4, 5, 6 and 8), in which *Y* denotes the rhenium loadings.

Catalyst characterization

Fourier transform infrared spectroscopy (FT-IR, Nexus Euro, Thermo Fisher Nicolet, USA) and ultra-violet-visible spectrophotometry (UV-Vis, U4100, Hitachi, Japan) were used to monitor the decomposition profiles of $Re_2(CO)_{10}$ during the microwave irradiation. The catalysts were soaked in *n*-octane for 24 h and then the solution was monitored by FT-IR and UV-Vis.

Powder X-ray diffraction (XRD) patterns of Re/C catalysts were obtained using a Rigaku XRD diffractometer (Rigaku D/Max-RB, Rigaku, Japan) using CuKα (λ = 1.54178 Å) as the radiation source, operated at 40 kV and 100 mA with a scan speed of 10° min^{-1}.

The contents of rhenium in Re/C catalysts were analyzed by inductively coupled plasma atomic emission spectroscopy (ICP, Optima 2000DV, PerkinElmer, USA). CO chemical adsorption was measured with an Autosorb-iQ (Quantachrome, USA). The catalysts were reduced for 1 h under hydrogen at 300 °C, then cooled to 30 °C and CO adsorption was measured.

Transmission electron microscopy (TEM) and high-resolution transmission electron microscopy (HRTEM) were performed with a Philips CM200 FEG TEM (Philips, Japan). The composition distribution analysis (HAADF-STEM and elemental mapping) was performed in STEM mode in combination with energy dispersive X-ray spectroscopy (EDX) using a DX4 analyzer system (EDAX) in the same microscope.

Temperature-programmed reduction (TPR) was carried out using a chemical adsorption instrument (Micromeritics Autochem 2910, Quantachrome, USA). The samples were firstly treated with inert gas for 1 h at 200 °C, and then the samples were heated to 800 °C at a speed of 10 °C min^{-1}. The gas mixture is composed of 10% hydrogen and 90% argon at a flow rate of 100 mL min^{-1}. The peak area of TPR profiles was used for quantitative analysis and the peak area of the Re/C-5 catalyst was used as the standard. The relative hydrogen consumption was calculated according to the following equation:

$$\text{Relative hydrogen consumption of Re/C-}X = \frac{\text{peak area of Re/C-}X}{\text{peak area of Re/C-5}}$$

Catalyst evaluation

Hydrogenation of succinic acid was performed in a Hastelloy alloy autoclave (50 mL) equipped with a magnetic stirrer, a heater and a controller. Before reaction, the catalysts were pretreated in a flow of hydrogen gas at 300 °C for 90 min. The reaction solution consisted of 18.0 g of deionized water, 2.0 g of succinic acid and 0.2 g of reduced catalyst. Then the autoclave was purged with H_2 to the desired pressure (typically 8.0 MPa), heated to the desired temperature (typically 240 °C) and maintained at that temperature for 10 h with continuous stirring (800 rpm min^{-1}). After reaction, the reactor was cooled to room temperature. The catalysts were filtered and dried at 120 °C for 4 h. The selectivity and conversion of the reaction product was analyzed by gas chromatography (Tianmei GC7890, China) and liquid chromatography (Waters 1525, USA), respectively.

Results and discussion

Characterization of Re/C catalysts

Fig. 1 shows the FT-IR and UV-Vis spectra of octane, $Re_2(CO)_{10}$ and supported rhenium catalysts with different microwave irradiation times. As shown in Fig. 1(a), the bands at 2071 cm^{-1}, 1975 cm^{-1}, 2017 cm^{-1} and 590 cm^{-1} are characteristic absorption peaks of $Re_2(CO)_{10}$. The bands at 2071 cm^{-1} and 1975 cm^{-1} are assigned to C═O horizontal stretching vibration in $Re_2(CO)_{10}$ and the band at 2017 cm^{-1} is assigned to C═O vertical stretching vibration in $Re_2(CO)_{10}$. The band at 590 cm^{-1} is caused by Re–C stretching vibration in $Re_2(CO)_{10}$.[27] The intensity of these characteristic peaks gradually disappeared with increasing irradiation time, indicative of the $Re_2(CO)_{10}$ decomposition into metallic Re. Most of the $Re_2(CO)_{10}$ were completely decomposed when irradiation time is above 3 minutes. From Fig. 1(b), the bands at 276 nm and 309 nm are ascribed to the existence of C═O in $Re_2(CO)_{10}$.[28] The results of UV-Vis in Fig. 1(b) are consistent with the results of FT-IR.

Fig. 2 shows the XRD patterns of supported rhenium catalysts at different microwave irradiation times and with different Re loadings. According to standard X-ray diffraction patterns (JCPDS no. 05-0702), diffraction peaks at $2\theta = 42.9$, 40.5 and 37.6° should be observed in these catalysts, which were indexed as the (101), (002) and (100) planes of metallic Re. However, Fig. 2(a) reveals that no discernible characteristic diffraction peak due to metallic Re was observed but the diffraction peaks of active carbon. This indicates that the rhenium particles are too small to be resolved (less than 4 nm) and/or highly dispersed on the surface of active carbon. In addition, the characteristic diffraction peaks of Re almost coincided with that of active carbon, which would also cover the peaks of Re. When increasing the Re loading of catalysts, no significant reflection was observed from XRD patterns in Fig. 2(b), indicating that the rhenium particles still exhibited well dispersion and small particle size at high Re loading.

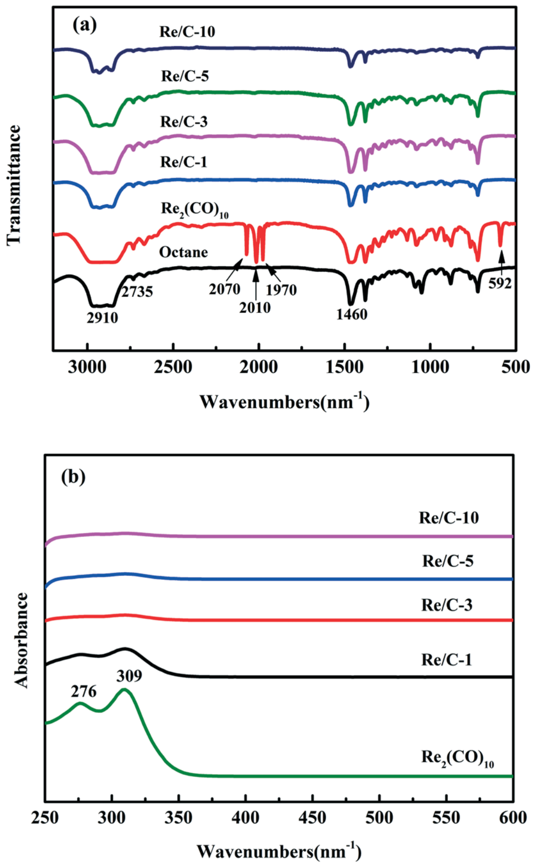

Fig. 1 FT-IR (a) and UV-Vis (b) spectra of liquid from Re/C-*X* (*X* = 1–10) dissolved in octane, $Re_2(CO)_{10}$ and octane.

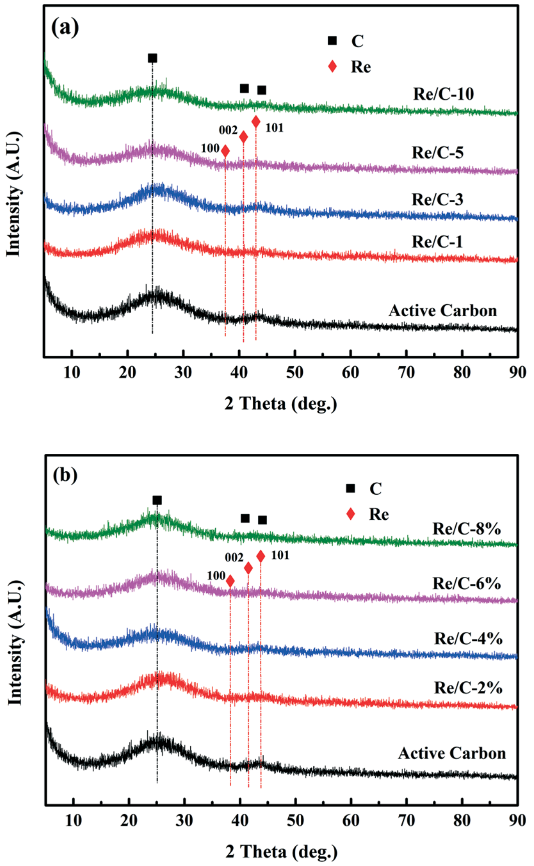

Fig. 2 XRD patterns of supported Re catalysts with different irradiation times and different Re loadings.

To further study the structure and composition distribution, Fig. 3 and Fig. S1† show the TEM, HRTEM images and STEM of supported Re catalysts. The TEM image in Fig. 3(a) confirmed that the metal particles were well dispersed on Re/C catalysts, and exhibited non-symmetrical shapes with particle size ranging from 1 to 4 nm. The catalysts prepared with 5 minutes microwave irradiation time (Re/C-5) showed better dispersion and smaller particle size than other catalysts (Re/C-7 and Re/C-10) in Fig. S1.† When increasing irradiation time, the agglomeration of particles took place as a result of the extra energy provided by the microwave irradiation. It can be seen from the particle size distribution in Fig. S1† that the particle size moderately increases with extended irradiation

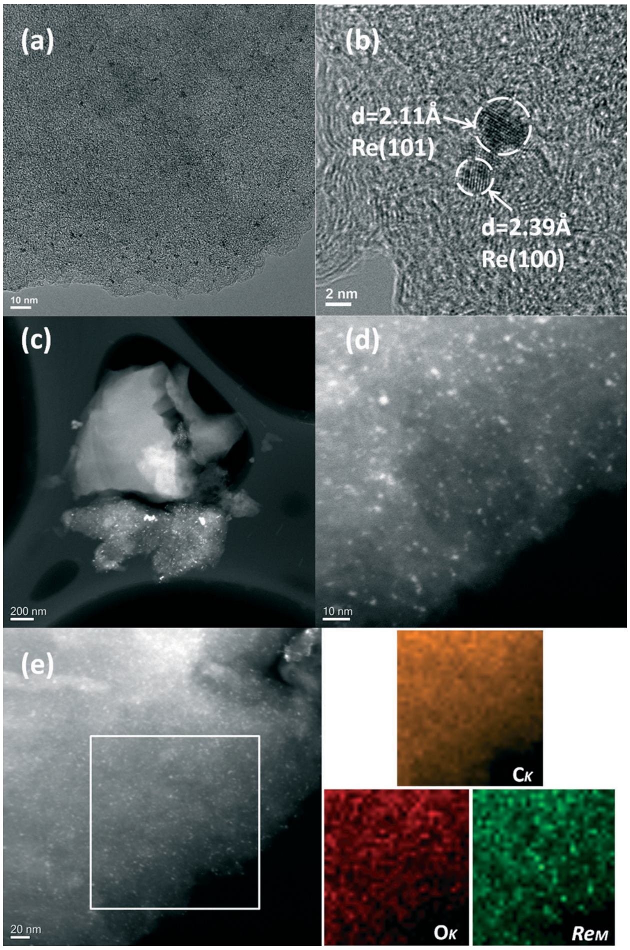

Fig. 3 TEM image (a), HRTEM image (b), HAADF-STEM (c), (d) and elemental mapping (e) of Re/C-5 catalyst which is pre-reduced by H_2.

time. The lattice spacing (2.11 Å and 2.39 Å) observed in HRTEM images clearly points to hexagonal rhenium ((101) with 2.11 Å and (100) with 2.39 Å based on JCPDS 05-0702; Fig. 3(b)).The phenomenon of agglomeration usually couldn't be avoided in the preparation process of catalysts, especially for the microwave-assisted thermolytic method which possesses a high-energy feature. However, most of rhenium particles are well dispersed on the Re/C catalyst and exhibit small non-symmetrical shapes except for a small number of larger nanoparticles caused by agglomeration of rhenium metallics from the images of HAADF-STEM (Fig. 3(c) and (d)). Combined with the results in Fig. S1,† the particle morphology could be adjusted by varying the microwave time in the microwave-assisted thermolytic method.

Homogeneous Re, C and O distributions in the sample are confirmed by the STEM dark field image and the corresponding elemental maps are shown in Fig. 3(e). The existence of oxygen may be due to the oxygen-containing groups on active carbon obtained from its pre-treating process by HNO_3 solution. Meanwhile the elemental maps also demonstrate the well dispersion of rhenium particles.

The results of CO chemical adsorption and ICP are shown in Table 1. The CO chemical adsorption indicates that there are more active sites on the surface of Re/C catalysts prepared by the microwave-assisted method than other Re/C catalysts[13] and rhenium particles exhibited good dispersion. The amounts of active sites firstly increased because more $Re_2(CO)_{10}$ decomposed into Re metal when increasing irradiation time and then decreased as a result of agglomeration of particles when prolonging irradiation time. But the phenomenon of agglomeration was only moderate after 7 minutes of irradiation since no obvious change was observed for CO adsorption capacity and dispersion. These results could also be verified by TEM images.

H_2-TPR tests were performed to investigate the change in reduction state of catalysts as a function of temperature. One peak was detected at around 370 °C in all catalysts prepared with different irradiation times from Fig. 4. This hydrogen consumption is assigned to the reduction of oxidized Re which is caused by re-oxidation of metallic rhenium after exposure to oxygen in the air.[29]

It was found that the reduction temperature didn't change with increasing microwave irradiation time, which demonstrated that the interaction between Re and supports was almost the same in these catalysts. As shown in Table 2, the catalysts with different irradiation times exhibited the same hydrogen consumption. It indicated that Re/C-*X* catalysts showed a similar phase state which was not influenced by the preparation conditions such as irradiation time. Besides, a broader peak was observed at high temperature, between 500 and 700 °C, which can be attributed to carbon methanation. The active carbon supports were pretreated with nitric acid solution to produce more functional groups on its surface, because of that, partial carbon on the surface of supports can easily react with hydrogen. Meanwhile, the existence of the Re phase might also enhance the reduction of functionalized carbon on the surface of catalysts.[30]

Table 1 CO-absorb and ICP results of supported Re catalysts

Catalysts	Re loading in theory (wt.%)	Actual Re loading (wt.%)	CO adsorption capacity (μmol g^{-1})	Dispersion[a] (%)
Active carbon	—	—	1.0	—
Re/C-3	4.0	4.0	45.0	20.9
Re/C-5	4.0	3.8	52.7	25.8
Re/C-7	4.0	3.9	45.1	21.5
Re/C-10	4.0	3.9	49.2	23.5

[a] Irreversible adsorption of CO calculated per each metal atom in Re/C catalyst.

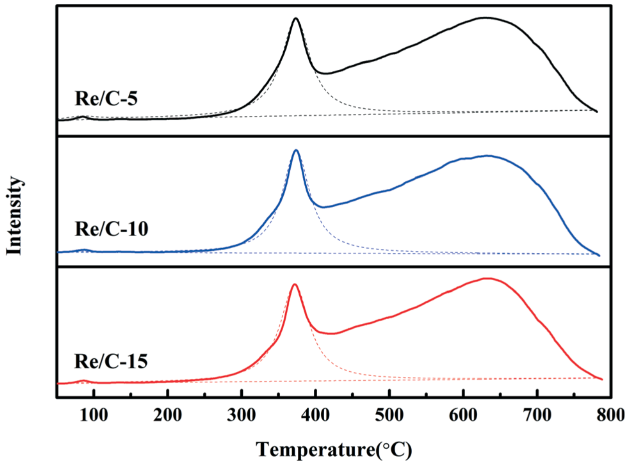

Fig. 4 H_2-TPR profiles of supported Re catalysts.

Table 2 Relative hydrogenation consumption of supported Re catalysts

	Re/C-5	Re/C-10	Re/C-15
Relative hydrogen consumption	1.00	1.01	0.99

Hydrogenation of succinic acid

Effects of microwave irradiation time and rhenium loading on catalytic performance. The activity of different catalysts in hydrogenation of succinic acid is summarized in Table 3. In the aqueous phase hydrogenation of succinic acid, the catalytic activity firstly increased and then decreased with increasing microwave irradiation time. The highest conversion of succinic acid (91.0%), with 59.2% selectivity to GBL and 33.0% selectivity to THF, was detected on Re/C-5. The variation in selectivity could be tuned by varying the amounts of active sites on catalysts. Increasing irradiation time until 5 min, there are more $Re_2(CO)_{10}$ that decomposed to Re metal, as already proven by CO chemical adsorption studies. However, the particles that agglomerate by overly prolonging irradiation time would decrease the amounts of active sites in return. From the results of CO chemical adsorption and TEM images, the influence of this phenomenon was not very obvious when further increasing irradiation time. Coincided with that, the conversion of succinic acid changed only little when irradiation time was above 7 minutes.

With increasing Re loading (from 2 wt.% to 8 wt.%), the conversion of succinic acid increased from 34.1% to 94.5% with the selectivity to GBL decreasing from 93.2% to 19.8% and the selectivity to THF increasing from 5.7% to 66.7%. The conversion of succinic acid had a great leap at 4 wt.% Re resulting from the lack of active sites when rhenium loading was very low. Furthermore, the change in conversion was small, compared to a significant change in selectivity when Re loading was above 4%. When the conversion of succinic acid was above 90%, the concentration of succinic acid was much lower than that of GBL and most of the active sites were occupied by it. The transformation of succinic acid then slowed down, resulting in a small change in conversion of succinic acid and increased selectivity to THF when Re loading was above 4 wt.%.

Effect of succinic acid concentration. The effects of succinic acid concentration on conversion and products are demonstrated in Table 4. High conversion (>90%) could be obtained even though the concentration was increased up to 10 wt.% which was higher than the concentration in industrial production to our knowledge.[6] The selectivity to GBL was improved with increasing succinic acid content in aqueous solution and the selectivity to THF was just the opposite. This phenomenon could be explained by investigating the reaction mechanism as shown in Scheme 1. Hydrogenation of succinic acid involves consecutive reaction steps and GBL was proposed to be the intermediate product.[13] The catalysts have sufficient active sites for hydrogenation of succinic acid and for further hydrogenation of GBL at low acid concentration. However, at high acid concentration, the reaction needs more active sites and most of active sites are occupied by succinic acid which suppressed further hydrogenation of GBL.

Effect of reaction temperature and pressure. From the results in Table 5, increasing temperature (from 200 °C to

Table 3 Hydrogenation of succinic acid on different catalysts

Catalyst	Reactant	Conversion (%)	Selectivity[a] (%) GBL	THF	BDO	NBA	NPA
Re/C-3	SUC	70.3	83.3	14.5	0.4	1.3	0.5
Re/C-4	SUC	72.3	82.6	15.1	0.6	1.3	0.4
Re/C-5	SUC	91.0	59.2	33.0	4.0	2.9	0.9
Re/C-7	SUC	78.5	78.1	19.3	0.5	1.4	0.7
Re/C-10	SUC	84.1	70.3	25.1	1.6	2.2	0.8
Re/C-15	SUC	82.6	75.2	21.6	1.2	1.6	0.4
Re/C-2%	SUC	34.1	93.2	5.7	0.2	0.5	0.4
Re/C-3%	SUC	48.4	90.0	8.5	0.3	0.7	0.5
Re/C-4%	SUC	91.0	59.2	33.0	4.0	2.9	0.9
Re/C-5%	SUC	92.3	41.8	44.5	8.4	3.7	1.6
Re/C-6%	SUC	92.9	43.6	45.4	5.9	4.0	1.1
Re/C-8%	SUC	94.5	19.8	66.7	7.1	5.0	1.4

[a] GBL = γ-butyrolactone; THF = tetrahydrofuran; BDO = 1,4-butanediol; NBA = *n*-butanol; NPA = *n*-propanol. Reaction conditions: 20 g solution (concentration = 10 wt.%), 0.2 g catalyst, 240 °C, 8.0 MPa, 800 rpm, 10 h.

Table 4 Effect of succinic acid concentration on conversion and product distribution over Re/C-5 catalysts[a]

Succinic acid concentration (wt.%)	Conversion (%)	Selectivity (%)				
		GBL	THF	BDO	NBA	NPA
5	95.5	17.7	65.5	9.9	5.3	1.6
7	91.4	52.5	38.1	5.8	2.8	0.8
10	91.0	59.2	33.0	4.0	2.9	0.9
12	77.1	79.2	18.2	0.5	1.7	0.4
15	69.6	82.4	15.6	0.7	1.0	0.3

[a] Reaction conditions: 20 g solution (concentration = weight of succinic acid × 100/weight of solution), 0.2 g catalyst, 240 °C, 8.0 MPa, 800 rpm, 10 h.

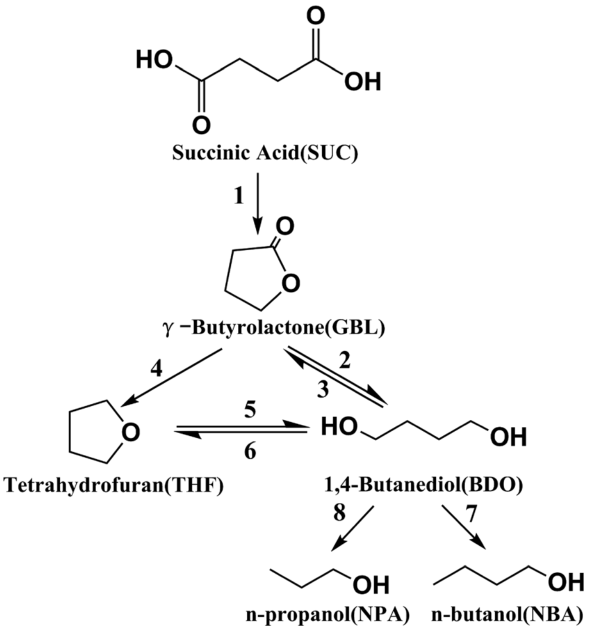

Scheme 1 Main reaction route of succinic acid catalytic hydrogenation with supported rhenium catalysts.

240 °C) would observably promote the conversion of SUC (from 46.2% to 91.0%) which was accompanied by the increase and decrease in the selectivity to THF (from 7.8% to 33.0%) and GBL (from 90.2% to 59.2%), respectively. For this consecutive reaction (Scheme 1), the transformation of intermediate product GBL was also simultaneously enhanced when the catalytic activity was improved by increasing temperature. Increasing pressure could exhibit a similar rule compared with increasing temperature, but the extent of the impact was much smaller. Besides that, not only was the succinic acid hydrogenolysis accelerated, but also could the by-products such as NBA and NPA be slightly increased with the increase in temperature and pressure. These results indicate that the catalyst can generate fewer by-products in the hydrogenation of succinic acid.

Kinetics of succinic acid hydrogenation. Our group has also studied the kinetic relationship between different reactants over supported rhenium catalysts. It was found that the conversion was 81.3% and the main products were THF (89.5%) and BDO (6.2%) when using GBL as the reactant; however, when the reactant was THF or BDO, less or no GBL was produced, as shown in Table 6. This indicates that SUC is firstly hydrogenated to GBL and then proceeds further to hydrogenation of GBL. From the results, the conversion was 93.6% and the main product was THF (93.1%) when using BDO as the reactant, compared to a very low conversion (1.7%) with THF as the reactant. The yield of NBA (0.6 and NPA (0%) was much lower when using THF as the reactant than the yield of NBA (4%) and NPA (0.6%) when BDO was used as the reactant. This shows that the main products of GBL hydrogenolysis are THF and BDO, at the same time BDO could be further hydrogenated to THF, NBA and NPA, on the contrary, THF could not be further converted to other products. The cyclodehydration of BDO to THF could be influenced by acidic properties of catalysts and by reaction temperature.[31,32] To remove impurities and modify the activated carbon, the activated carbon was pre-treated with HNO_3 solution which increases the functional groups such as hydroxyl groups on the surface of Re/C catalysts.[33] The graft of functional groups onto the surface of active carbon could increase the acidity of support and promoted the cyclodehydration of BDO to THF. In addition to the influence of acidity, the high temperature (above 200 °C) could also accelerate cyclodehydration of BDO in our experiment. The effortless cyclodehydration of BDO was proved by the results above. A reasonable reaction route is shown in Scheme 1.

The time course of succinic acid hydrogenolysis is shown in Fig. 5. The relative concentration of SUC decreased with increasing reaction time. The reaction rate of succinic acid decreased after 10 h as a result of its lowered concentration. The relative concentration of GBL increased firstly, then passed a maximum and gradually dropped. When reaction time was below 3 h, it was found that the consumption rate

Table 5 Hydrogenation of succinic acid over Re/C-5 in different reaction conditions[a]

Reaction conditions		Conversion (%)	Selectivity (%)				
Temperature (°C)	Pressure (MPa)		GBL	THF	BDO	NBA	NPA
200	8.0	46.2	90.2	7.8	0.8	0.8	0.4
220	8.0	70.1	82.6	14.9	1.1	1.1	0.3
240	8.0	91.0	59.2	33.0	4.0	2.9	0.9
240	7.0	85.6	69.4	26.6	1.1	2.1	0.8
240	6.0	80.3	79.2	17.6	1.0	1.7	0.5

[a] Reaction conditions: 20 g solution (concentration of SUC = 10 wt.%), 0.2 g catalyst, 800 rpm, 10 h.

Table 6 Hydrogenation of succinic acid and its hydrogenated products over supported Re catalysts[a]

Catalyst	Reactant	Conversion (%)	Selectivity (%)					
			SUC	GBL	THF	BDO	NBA	NPA
Re/C-5	SUC	91.0	—	59.2	33.0	4.0	2.9	0.9
Re/C-5	GBL	81.3	0	—	89.5	6.2	3.4	0.9
Re/C-5	BDO	93.6	0	2.2	93.1	—	4.1	0.6
Re/C-5	THF	1.7	0	0	—	62.6	37.4	0

[a] Reaction conditions: 20 g solution (concentration = 10 wt.%), 0.2 g catalyst, 240 °C, 8.0 MPa, 800 rpm, 10 h.

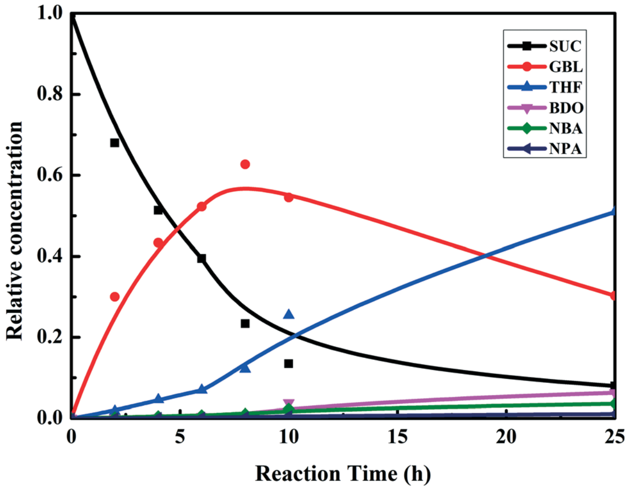

Fig. 5 Time course of succinic acid hydrogenolysis over Re/C-5 catalysts. (Reaction conditions: 20 g solution (concentration = 10 wt.%), 0.2 g catalyst, 240 °C, 8.0 MPa, 800 rpm).

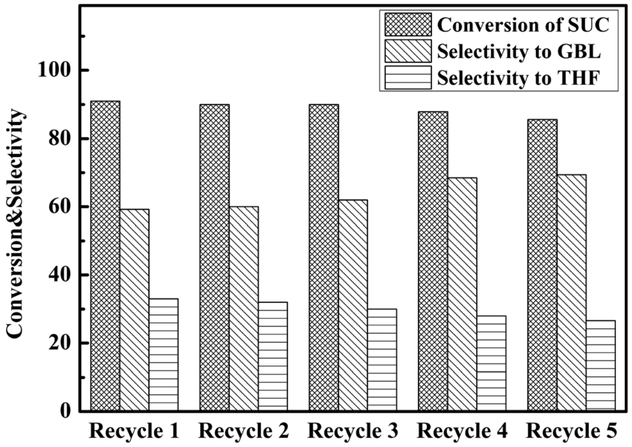

Fig. 6 Aqueous hydrogenation of succinic acid over Re/C-5 catalysts with respect to recycle run.

of SUC was equal to the production rate of GBL, which was almost the only product. Combined with Scheme 1, step 1 was firstly accelerated. When the reaction proceeded to above 20 h (SUC was almost completely consumed), the consumption rate of GBL was equal with the production rate of BDO and THF. By increasing concentration of GBL, step 2 and step 4 are activated. THF is the main final product because of the fact that BDO could be easily hydrogenated to THF (step 6). That is also the reason why the selectivity or relative concentration of THF continues to increase with increasing pressure, temperature, time and active sites. All these results show that GBL is an intermediate product which could achieve a maximum yield when reaction time is appropriate, and THF is the final product whose yield could exceed 40% accompanied by less by-products when extending the reaction time. In conclusion, the product distribution could also be adjusted by varying the reaction time at a certain scope from the results of kinetic studies.

Stability of Re/C catalyst. To investigate the stability and reusability of the catalyst, recycle tests for hydrogenation of succinic acid over Re/C-5 catalysts were performed for five times in our experiment. After reaction, most of the reaction liquid was separated from the catalyst by centrifugation and only a little part was left to protect catalysts from oxidation. Then, the fresh reaction liquid, separated catalysts and a small amount of fresh catalysts which were used to make up for the loss of catalysts were added into the autoclave reactor.

Fig. 6 shows the result for aqueous hydrogenation of succinic acid over Re/C-5 catalysts with respect to recycle run. A slight drop of catalytic activity was detected in our experiment after five times recycle. No significant leaching of rhenium was detected by ICP-AES analysis from the result in Table S1.† It indicates that the Re/C-5 catalysts prepared with the microwave-assisted method which relies on the thermolytic effect of microwave irradiation could serve as a stable catalyst in the aqueous hydrogenation of succinic acid.

Conclusions

The supported rhenium catalysts can be prepared by the microwave-assisted thermolytic method. The use of organic solvents can be avoided and thus this method provides a route to a more environmentally friendly process. The catalysts exhibit good dispersion of rhenium nanoparticles and efficient performance for the catalytic hydrogenation of succinic acid in aqueous solution. The catalytic properties of Re/C can be modified by changing Re loading, leading to improved conversion and selectivity. The agglomeration of Re particles caused by the thermal effect due to extra energy results in a decreased activity of Re/C catalysts. In addition, the catalytic hydrogenation of succinic acid on supported rhenium catalysts (Re/C-5) is a consecutive reaction and exhibits certain conversion relationship between different substances. Further studies demonstrated that different product distributions could be obtained by the variation of reaction time. According to our research in the past[13] and the literature,[12,15,16,19] Re/C catalysts prepared with the microwave-assisted thermolytic method exhibit more superior transformation performance of GBL which is the intermediate product to Pd based catalysts, and generate fewer by-products than Ru based catalysts when used for hydrogenation of succinic acid.

Acknowledgements

We gratefully acknowledge the financial support provided by the National Natural Science Foundation of China (no. 21428301 and 21373038), the Fundamental Research Funds for the Central Universities (DUT13RC(3)41) and the Postdoctoral Science Foundation of China (2013M541220). We thank Dr. Bingsen Zhang, from the Institute of Metal Research, Chinese Academy of Sciences, for technical support in HRTEM and STEM test.

Notes and references

1 A. Corma, S. Iborra and A. Velty, *Chem. Rev.*, 2007, **107**, 2411–2502.

2 C. Delhomme, D. Weuster-Botz and F. E. Kühn, *Green Chem.*, 2009, **11**, 13–26.

3 A. Cukalovic and C. V. Stevens, *Biofuels, Bioprod. Biorefin.*, 2008, **2**, 505–529.

4 J. G. Zeikus, M. K. Jain and P. Elankovan, *Appl. Microbiol. Biotechnol.*, 1999, **51**, 545–552.

5 J. C. Serrano-Ruiz, R. Luque and A. Sepulveda-Escribano, *Chem. Soc. Rev.*, 2011, **40**, 5266–5281.

6 M. Patel, M. Crank, V. Dornburg, B. Hermann, L. Roes, B. Hüsing, L. Overbeek, F. Terragni and E. Recchia, *The BREW project*, European Commission's GROWTH Programme, Utrecht, 2006.

7 U. Herrmann and G. Emig, *Ind. Eng. Chem. Res.*, 1997, **36**, 2885–2896.

8 U. Herrmann and G. Emig, *Ind. Eng. Chem. Res.*, 1998, **37**, 759–769.

9 P. Gallezot, *Chem. Soc. Rev.*, 2012, **41**, 1538–1558.

10 U. G. Hong, S. Hwang, J. G. Seo, J. Yi and I. K. Song, *Catal. Lett.*, 2010, **138**, 28–33.

11 S. H. Chung, Y. M. Park, M. S. Kim and K. Y. Lee, *Catal. Today*, 2012, **185**, 205–210.

12 B. Tapin, F. Epron, C. Especel, B. K. Ly, C. Pinel and M. Besson, *ACS Catal.*, 2013, **3**, 2327–2335.

13 Z. Shao, C. Li, X. Di, Z. Xiao and C. Liang, *Ind. Eng. Chem. Res.*, 2014, **53**, 9638–9645.

14 U. G. Hong, H. W. Park, J. Lee, S. Hwang and I. K. Song, *J. Ind. Eng. Chem.*, 2012, **18**, 462–468.

15 U. G. Hong, J. K. Kim, J. Lee, J. K. Lee, J. H. Song, J. Yi and I. K. Song, *Appl. Catal., A*, 2014, **469**, 466–471.

16 U. G. Hong, J. K. Kim, J. Lee, J. K. Lee, J. H. Song, J. Yi and I. K. Song, *J. Ind. Eng. Chem.*, 2014, **20**, 3834–3840.

17 R. M. Deshpande, V. V. Buwa, C. V. Rode, R. V. Chaudhari and P. L. Mills, *Catal. Commun.*, 2002, **3**, 269–274.

18 D. P. Minh, M. Besson, C. Pinel, P. Fuertes and C. Petitjean, *Top. Catal.*, 2010, **53**, 1270–1273.

19 L. Corbel-Demailly, B. K. Ly, D. P. Minh, B. Tapin, C. Especel, F. Epron, A. Cabiac, E. Guillon, M. Besson and C. Pinel, *ChemSusChem*, 2013, **6**, 2388–2395.

20 B. K. Ly, D. P. Minh, C. Pinel, M. Besson, B. Tapin, F. Epron and C. Especel, *Top. Catal.*, 2012, **55**, 466–473.

21 M. A. Ryashentseva, *Russ. Chem. Rev.*, 1998, **67**, 157–177.

22 U. G. Hong, H. W. Park, J. Lee, S. Hwang, J. Yi and I. K. Song, *Appl. Catal., A*, 2012, **415–416**, 141–148.

23 A. de la Hoz, A. Diaz-Ortiz and A. Moreno, *Chem. Soc. Rev.*, 2005, **34**, 164–178.

24 H. J. Kitchen, S. R. Vallance, J. L. Kennedy, N. Tapia-Ruiz, L. Carassiti, A. Harrison, A. G. Whittaker, T. D. Drysdale, S. W. Kingman and D. H. Gregory, *Chem. Rev.*, 2014, **114**, 1170–1206.

25 M. B. Gawande, S. N. Shelke, R. Zboril and R. S. Varma, *Acc. Chem. Res.*, 2014, **47**, 1338–1348.

26 X. Ni, B. Zhang, C. Li, M. Pang, D. Su, C. T. Williams and C. Liang, *Catal. Commun.*, 2012, **24**, 64–69.

27 D. M. Adams and I. D. Taylor, *J. Chem. Soc., Faraday Trans. 2*, 1982, **78**, 1065–1090.

28 S. Zhang, T. L. Brown, Y. Du and J. R. Shapley, *J. Am. Chem. Soc.*, 1993, **115**, 6705–6709.

29 S. R. Bare, S. D. Kelly, F. D. Vila, E. Boldingh, E. Karapetrova, J. Kas, G. E. Mickelson, F. S. Modica, N. Yang and J. J. Rehr, *J. Phys. Chem. C*, 2011, **115**, 5740–5755.

30 S. G. Wettstein, J. Q. Bond, D. M. Alonso, H. N. Pham, A. K. Datye and J. A. Dumesic, *Appl. Catal., B*, 2012, **117–118**, 321–329.

31 H. Li, H. Yin, T. Jiang, T. Hu, J. Wu and Y. Wada, *Catal. Commun.*, 2006, **7**, 778–782.

32 M. Aghaziarati, M. Kazemeini, M. Soltanieh and S. Sahebdelfar, *Ind. Eng. Chem. Res.*, 2006, **46**, 726–733.

33 J. Noh and J. Schwarz, *Carbon*, 1990, **28**, 675–682.